

Electronic Supplementary Information

A Facile Approach to Hetero-nanorods of Ag₂Se-MSe (M = Cd, Zn) with Enhanced Third-Order Optical Nonlinearity

Zhipeng Huang,*^a Maoying Li,^a Ding Jia,^a Peng Zhong,^a Feng Tian,^b Zhongzhong Chen,^a Mark G. Humphrey^c and Chi Zhang*^a

^a *Functional Molecular Materials Research Centre, Scientific Research Academy, Jiangsu University, Zhenjiang 212013, P. R. China. Fax/Tel: 86-511-88797815; E-mail: zphuang@ujs.edu.cn,*

^b *School of Materials Science and Engineering, University of Shanghai for Science and Technology, Shanghai 200093, P. R. China*

^c *Research School of Chemistry, Australian National University, Canberra, ACT 0200, Australia*

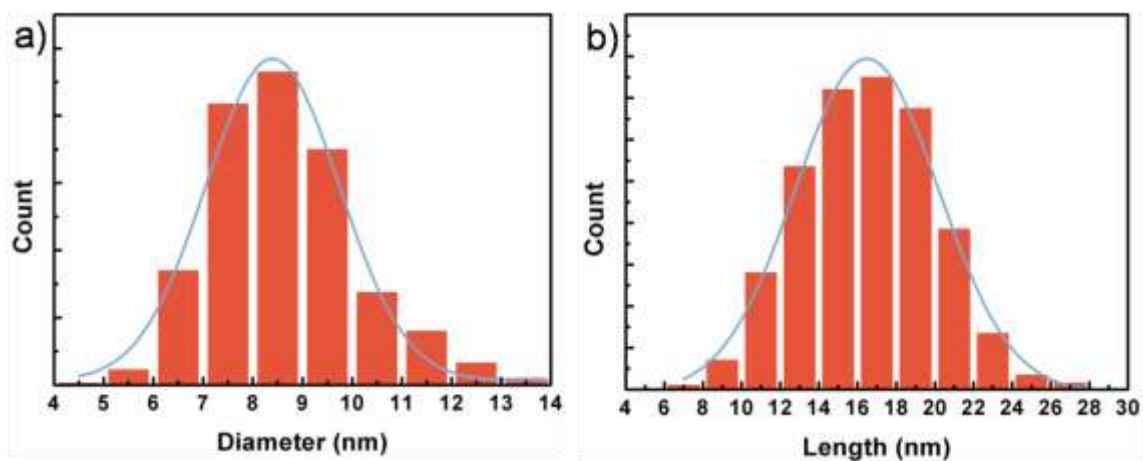


Figure S1. (a) Diameter and (b) length distribution of CdSe nanorods shown in Figure 1a. The blue solid lines show results of Gaussian fitting.

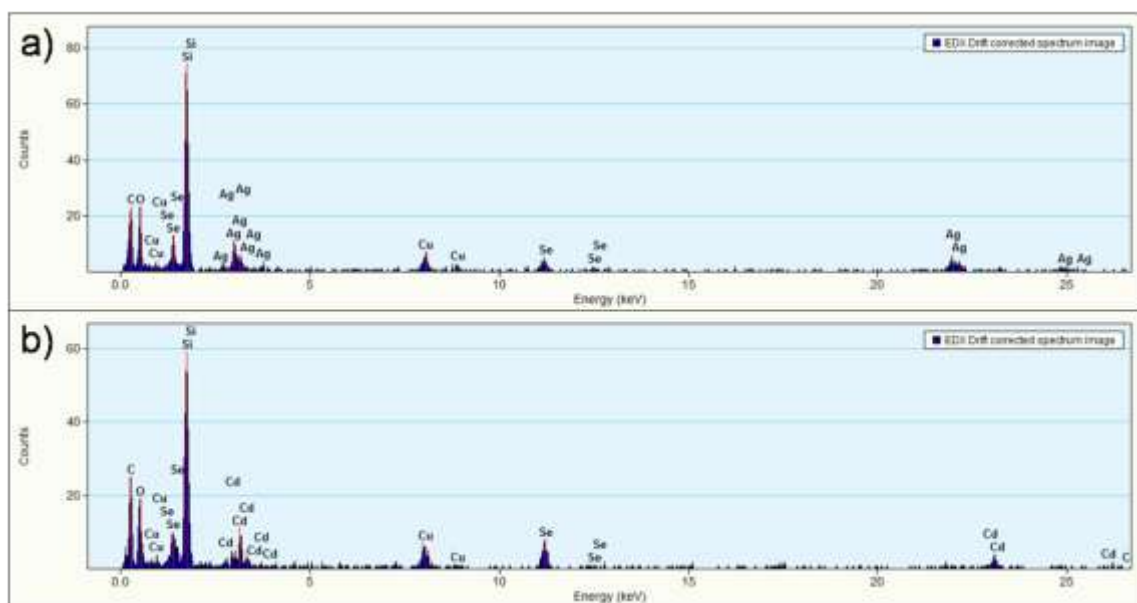


Figure S2. EDX spectra acquired respectively from the (a) hemispherical head (Ag_2Se portion) and (b) rod-like stick (CdSe portion).

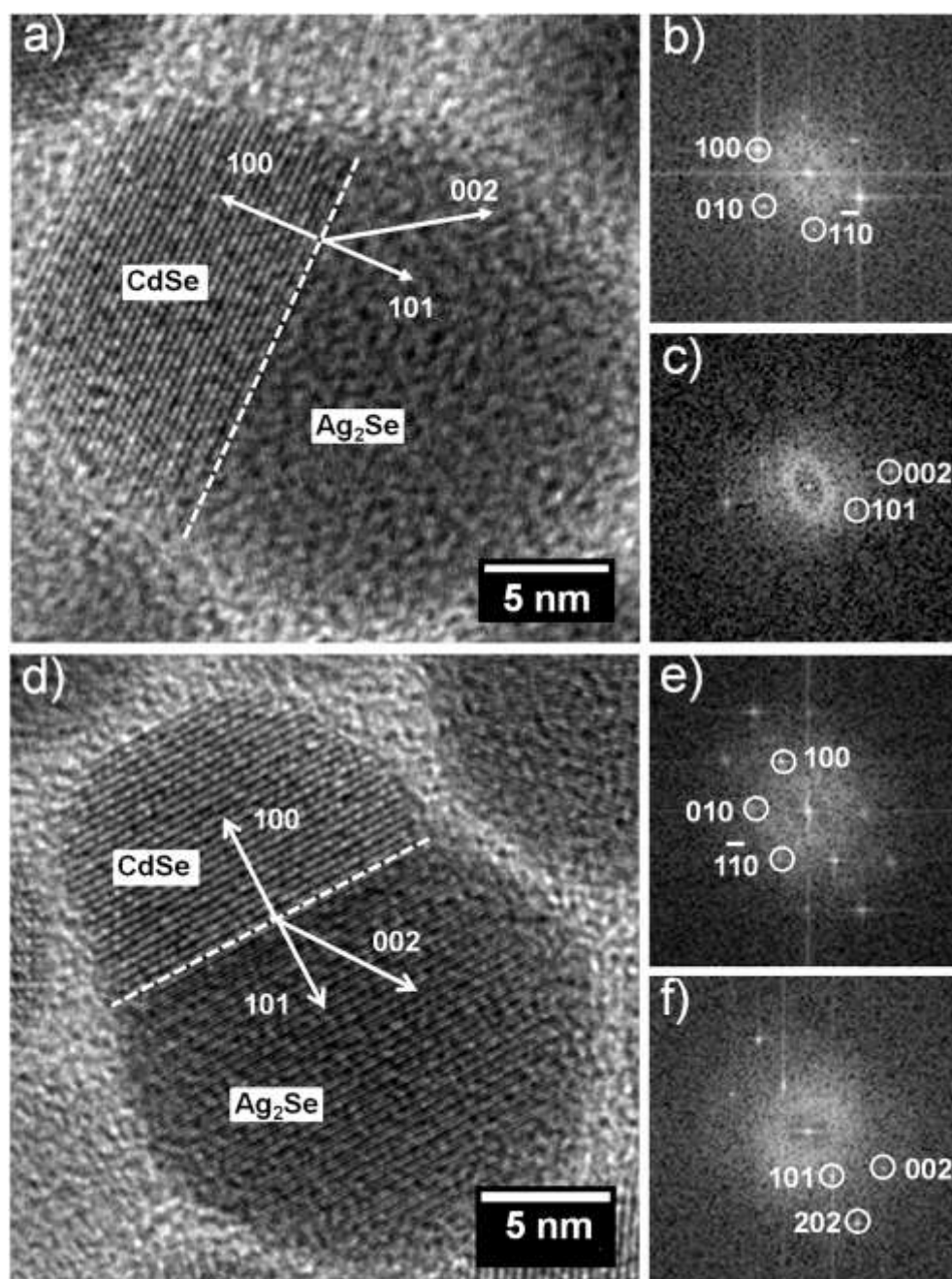


Figure S3. Epitaxial relationship revealed by HRTEM. (a, d) HRTEM images of different Ag_2Se - CdSe nano-heterojunction particles. (b) FFT from the CdSe component in the particle shown in (a). (c) FFT from the Ag_2Se component in the particle shown in (a). (e) FFT from the CdSe component in the particle shown in (d). (f) FFT from the Ag_2Se component in the particle shown in (d). The directions in (a) and (d) were drawn according to the FFT patterns from the corresponding components. As shown by (a) and (d), the epitaxial relationships between CdSe and Ag_2Se in the two particles can both be established as $(202)_{\text{Ag}_2\text{Se}} \parallel (100)_{\text{CdSe}}$ with $[010]_{\text{Ag}_2\text{Se}} \parallel [001]_{\text{CdSe}}$.

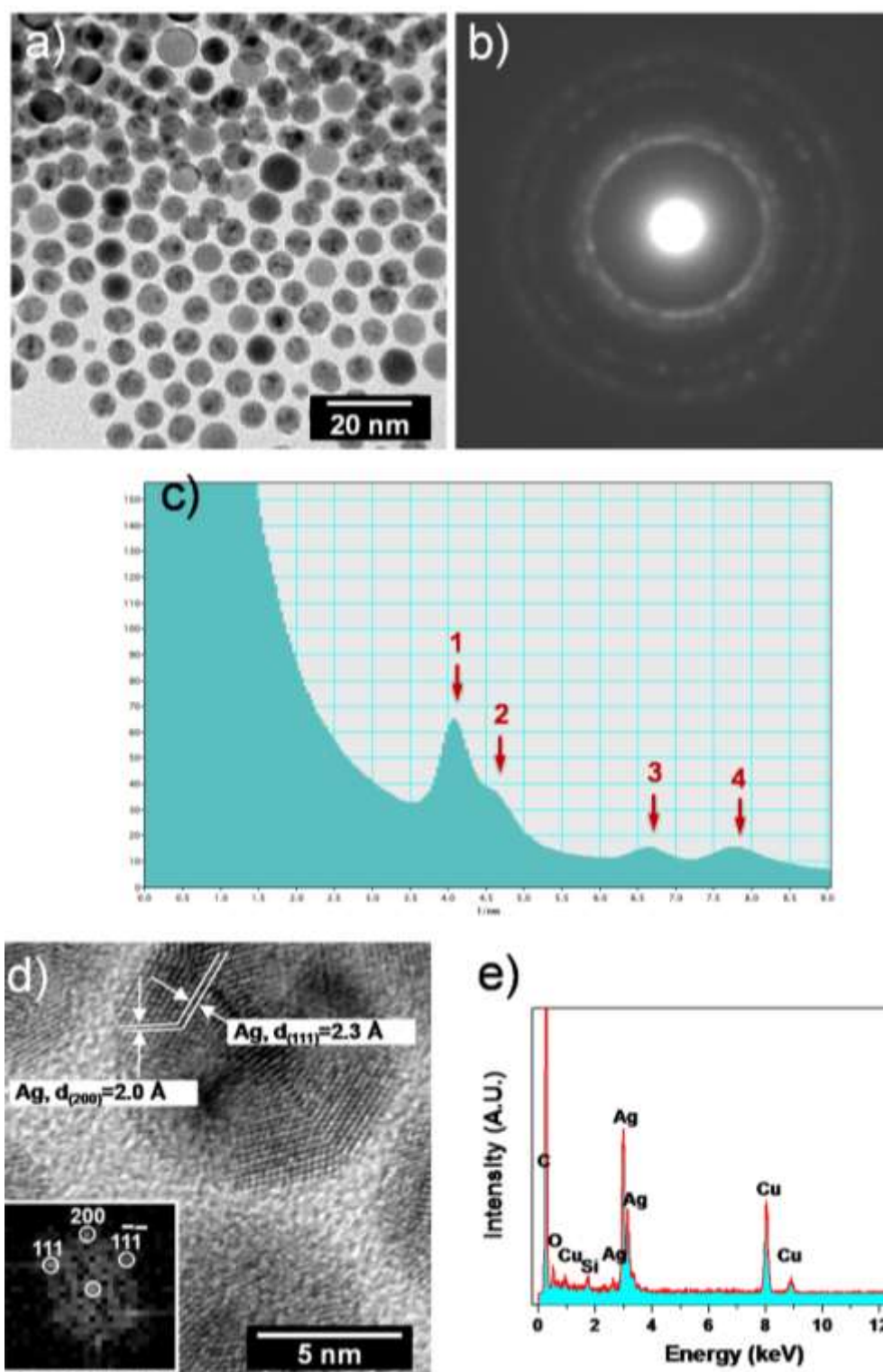


Figure S4. (a) TEM image of Ag particles extracted from growth solution prior to the addition of Se powder. (b) Selected area electron diffraction (SAED) patterns from Ag particles. (c) the corresponding rotation average of peak intensity vs reciprocal position from the center extracted from (b). The corresponding d-spacing derived from reciprocal position of peaks in (c) is listed in Table S1. The listed d-spacing matches well that of cubic phase Ag, suggesting that the diffraction patterns in (b) can be indexed by cubic phase Ag (JCPDS#4-783). (d) HRTEM image of Ag particles. (e) EDS spectrum of Ag particles.

Table S1. The measured reciprocal position of peaks shown in Figure S2, the corresponding measured d-spacing, the d-spacing from cubic phase Ag, and the resulting index of planes.

Peak Number	Reciprocal Position (1/nm)	D-spacing Measured (nm)	D-spacing of tetragonal Ag	Index of Plane
1	4.147	0.241	0.23590	111
2	4.766	0.209	0.20440	200
3	6.665	0.150	0.14450	220
4	7.827	0.128	0.12310	311

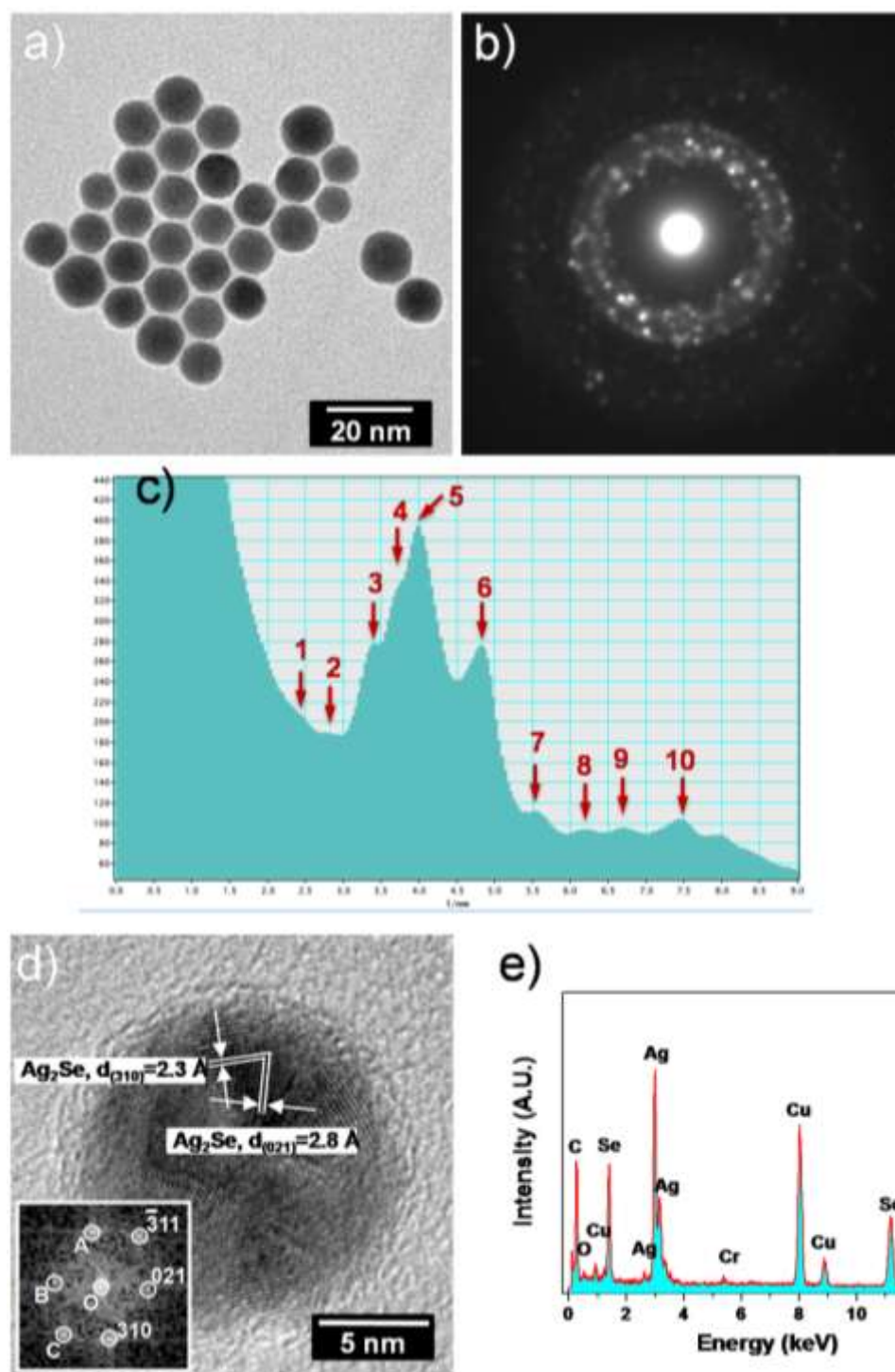


Figure S5. (a) TEM image of Ag₂Se particles extracted from growth solution prior to the addition of Cd(NO₃)₂ and Se powder. (b) Selected area electron diffraction (SAED) patterns from Ag₂Se particles. (c) the corresponding rotation average of peak intensity vs reciprocal position from the center extracted from (b). The corresponding d-spacing derived from reciprocal position of peaks in (c) is listed in Table S2. The listed d-spacing matches well that of tetragonal phase Ag₂Se.[1] (d) HRTEM image of Ag₂Se particles. (e) EDS spectrum of Ag₂Se particles.

Table S2. The measured reciprocal position of peaks shown in Figure S3, the corresponding measured d-spacing, the d-spacing from tetragonal phase Ag₂Se,^[1] and the resulting index of planes.

Peak Number	Reciprocal Position (1/nm)	D-spacing Measured (nm)	D-spacing of tetragonal Ag ₂ Se ^[1]	Index of Plane
1	2.441	0.409	0.40694582	101
2	2.829	0.353	0.3525688	111
3	3.41	0.293	0.287988434	201
4	3.72	0.269	0.266656511	211
5	3.991	0.251	0.249608694	220
6	4.844	0.206	0.212772345 0.203721559	301 311
7	5.58	0.179	0.182228957	321
8	6.2	0.161	0.161925976	411
9	6.742	0.148	0.143994217	402
10	7.44	0.134	0.135845137	501

[1] A. Sahu, L. J. Qi, M. S. Kang, D. N. Deng, D. J. Norris, *J. Am. Chem. Soc.* **2011**, *133*, 6509

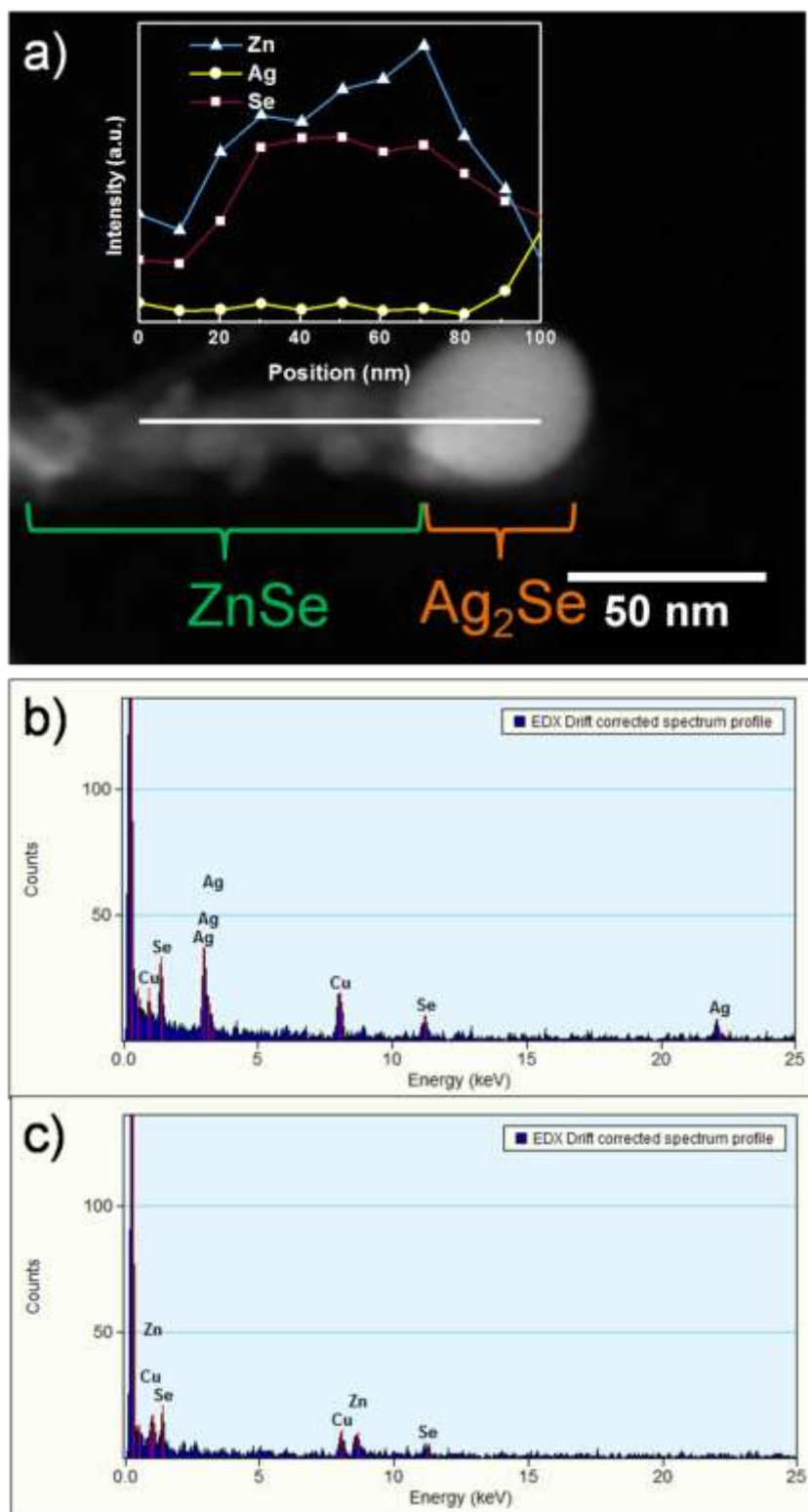


Figure S6. (a) HADIFF-STEM image of a single Ag₂Se-ZnSe hetero-nanorod. The inset shows line profiles of Zn (\triangle), Ag (\circ), and Se (\square) acquired along the thick white line. (b) and (c) show the EDX spectrum recorded from Ag₂Se and ZnSe part of Ag₂Se-ZnSe hetero-nanorod, respectively.

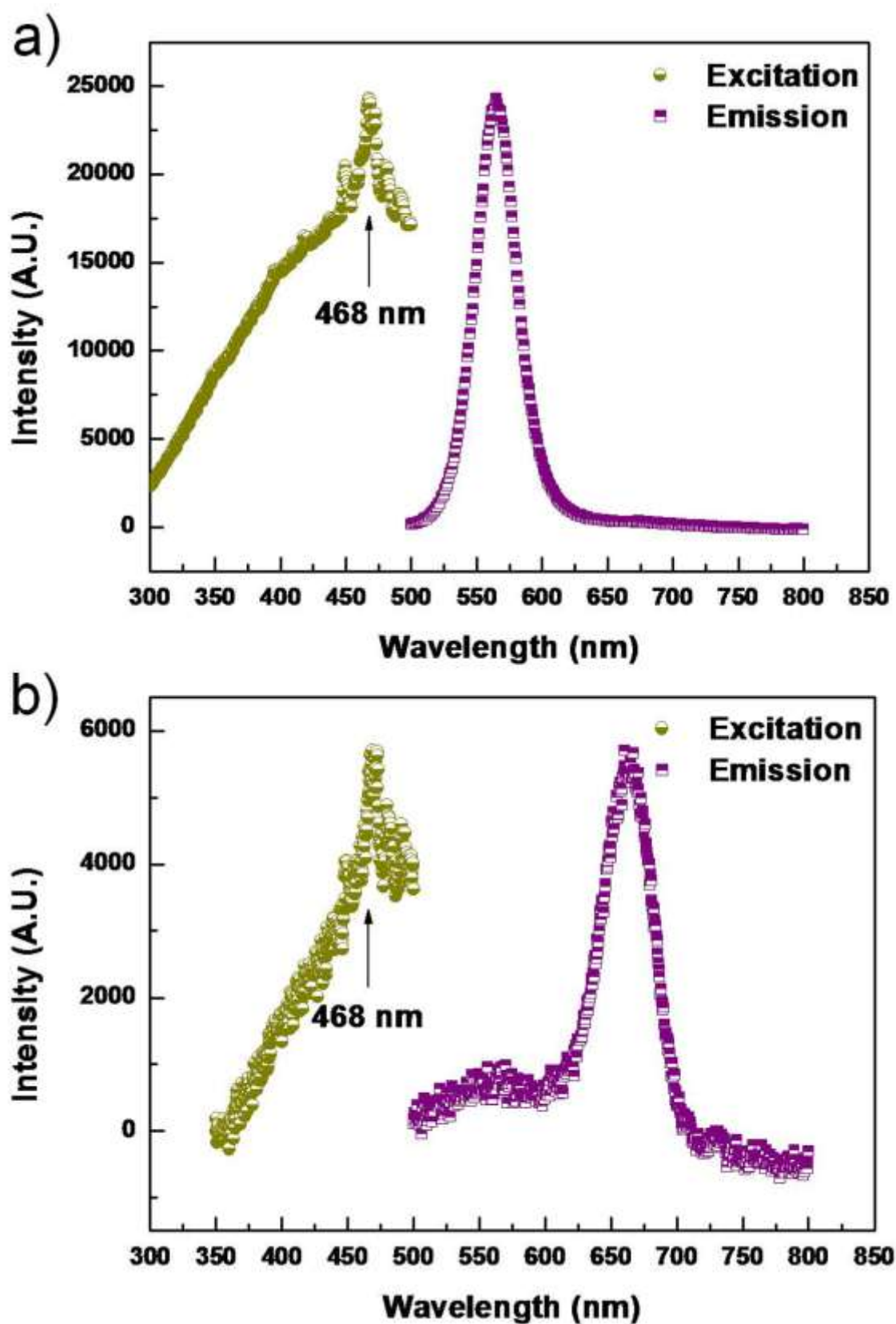


Figure S7. Excitation and emission spectra of (a) single component CdSe nanocrystals and (b) Ag₂Se-CdSe SSHNs.

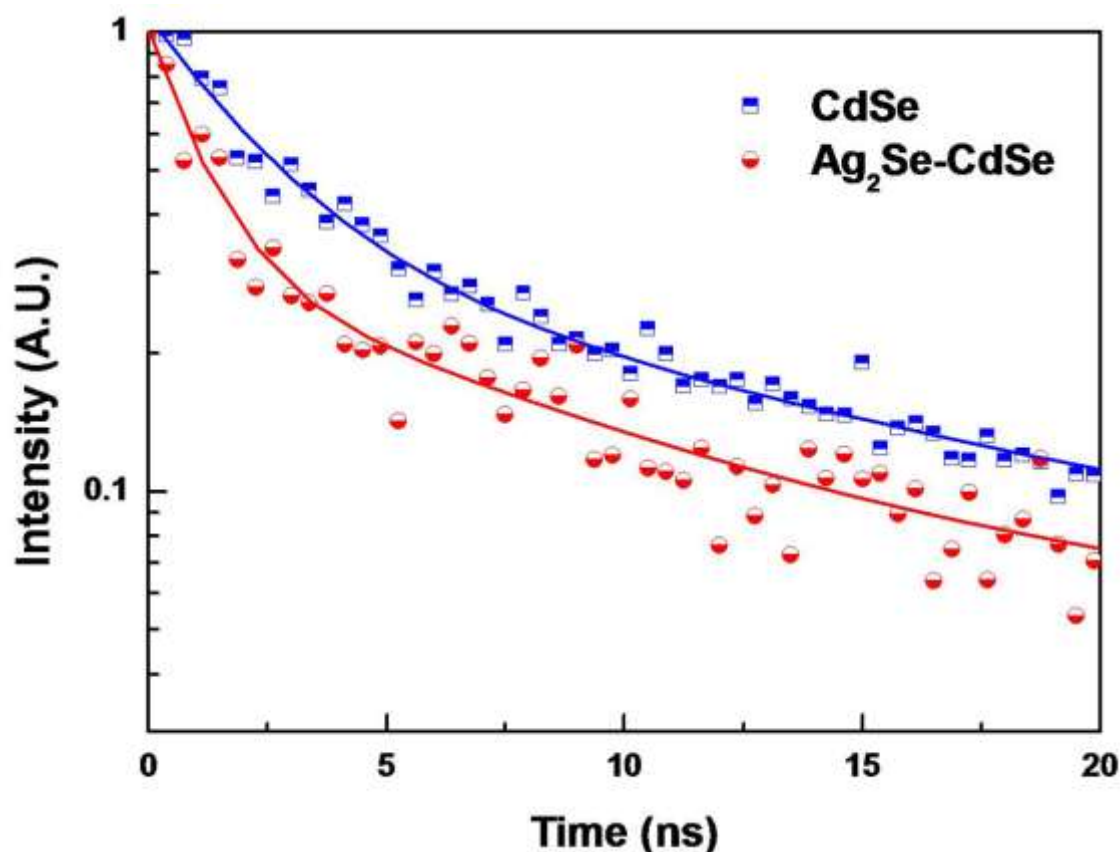


Figure S8. Plot of time-resolved fluorescence for single component CdSe nanocrystals and Ag₂Se-CdSe SSHNs vs elapsed time. The samples were excited by 481 nm laser (the available laser with wavelength closest to the excitation peak of samples), and the PL intensities were monitored at the strongest emission peak of each sample, 560 nm for single component CdSe nanocrystals and 668 nm for Ag₂Se-CdSe SSHNs. The solid lines are fits to the data using a three-exponential-decay function. The fitting results and the average lifetimes are listed in Table S3.

Table S3. The decay lifetimes derived from the fitting results of time-resolved fluorescence using a three-exponential-decay function. The average lifetime was calculated by the equation: $\tau_{\text{average}} = \sum_i A_i \tau_i / \sum_i A_i$.

	τ_1 (ns)	A_1	τ_2 (ns)	A_2	τ_3 (ns)	A_3	τ_{average} (ns)
CdSe	2.27189	0.73675	12.98703	0.27583	88.14526	0.07617	10.99431
Ag ₂ Se-CdSe	1.05601	0.38886	1.05655	0.30723	8.93259	0.27141	3.26578

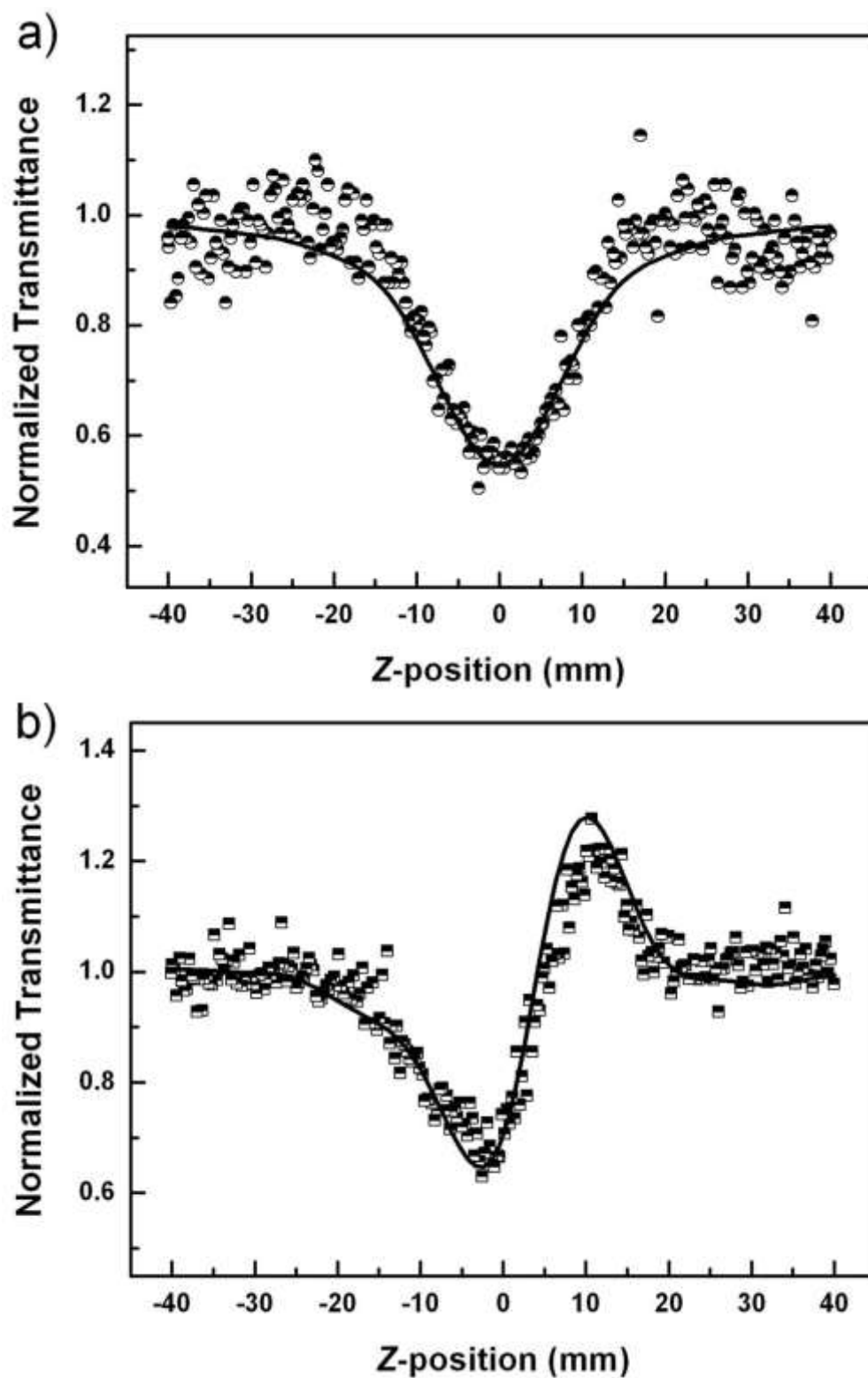


Figure S9. Z-scan results of $\text{Ag}_2\text{Se-ZnSe}$ nano-heterojunctions dispersed in toluene with a linear transmittance of 85% (4 ns, 532 nm laser pulses). The half-open circles/squares represent the Z-scan experimental data, and the solid lines are the theoretical fitting curves: (a) data collected under the open-aperture configuration; (b) data obtained by dividing the normalized Z-scan data obtained under the closed-aperture configuration by the normalized Z-scan data in (a).

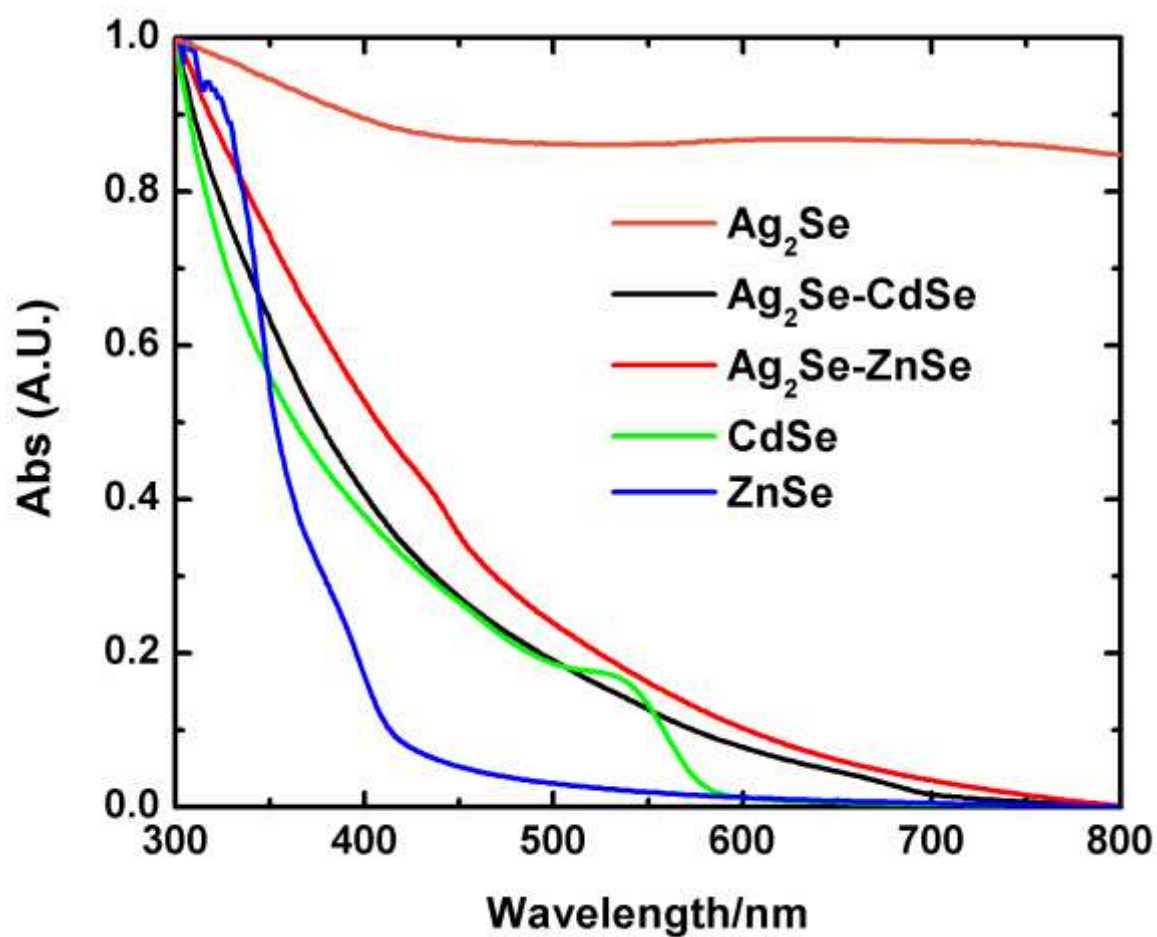


Figure S10. UV-Vis spectra of SSHNs (Ag₂Se-CdSe and Ag₂Se-ZnSe) and single component nanocrystals (Ag₂Se, CdSe and ZnSe) dispersed in toluene.

Data Fitting

A model was developed by Li et al ^[1] to fit the Z-scan data taking into consideration the free carrier absorption:

$$dI/dz' = -(\alpha_0 + \beta I + \sigma_a N)I$$

$$dN/dt = \alpha_0 I / \hbar \omega + \beta I^2 / 2 \hbar \omega - N / \tau$$

where I is the intensity of laser, Z' is the position of sample, α_0 is linear absorption cross-section, β is two photon absorption coefficient, and σ_a is free carrier absorption cross-section, N is the carrier density, and τ is the carrier lifetime.

In our experiments, the band gap energy of CdSe, Ag₂Se-CdSe and Ag₂Se-ZnSe is smaller than the energy of single photon (2.33 eV, 532 nm), therefore, no two-photon absorption would be occur during the NLO measurement. Accordingly, the abovementioned model should be revised as:

$$dI/dz' = -(\alpha_0 + \sigma_a N)I$$

$$dN/dt = \alpha_0 I / \hbar \omega - N / \tau$$

In addition, the τ values of different samples were extracted from PL measurement (Table S3) and used as known values in the fitting of NLO data.

Ref:

[1] H.P. Li, C.H. Kam, Y.L. Lam, W. J. *Opt. Comm.* **2001**, *190*, 351.